International Journal of Pharmaceutics 413 (2011) 194–201

Contents lists available at ScienceDirect

International Journal of Pharmaceutics

journal homepage: www.elsevier.com/locate/ijpharm

Pharmaceutical Nanotechnology

Docetaxel-loaded-lipid-based-nanosuspensions (DTX-LNS): Preparation, pharmacokinetics, tissue distribution and antitumor activity

Lili Wang, Zhihong Liu, Donghua Liu, Chunxi Liu, Zhang Juan, Na Zhang*

School of Pharmaceutical Science, Shandong University, 44 Wenhua Xi Road, Ji'nan 250012, Shandong Province, China

ARTICLE INFO

Article history:
Received 21 January 2011
Received in revised form 12 April 2011
Accepted 13 April 2011
Available online 21 April 2011

Keywords:
Docetaxel
Lipid-based-nanosuspensions (DTX-LNS)
Antitumor activity

ABSTRACT

The purpose of the study was to design lipid-based-nanosuspensions (LNS) for Docetaxel (DTX) without Tween 80 for clinical intravenous administration (i.v.). DTX-LNS were prepared by high pressure homogenization method, and then lyophilization was carried out to improve the stability. The physical–chemical properties in terms of particle size, size distribution, zeta potential and morphology were evaluated, respectively. The *in vitro* cytotoxic activity was assessed by MTT against SKOV-3 and malignant melanoma B16 cells. The *in vivo* pharmacokinetics, tissue distribution as well as antitumor efficacy were investigated in B16 melanoma-bearing Kunming mice. The particle size and zeta potential of DTX-LNS were (200.0 ± 3.42) nm and (-11.15 ± 0.99) mV, respectively. Compared with Duopafei®, it was shown that DTX-LNS exhibited higher antitumor efficacy by reducing tumor volume ($P < 0.05$) and increasing survival rate in B16 melanoma-bearing mice and strongly reduced the anticancer drug toxicity. The results of biodistribution studies clearly indicated the superiority of DTX-LNS to Duopafei® in increasing the accumulation of DTX within tumor and the organs rich in macrophages (liver, lungs and spleen), while, the drug concentration in heart and kidney decreased. Together these results suggested that DTX-LNS could effectively inhibit tumor growth, reduce toxicity during the therapeutic procedure and hold the potential to be an appropriate choice for the clinical administration of DTX.

1. Introduction

During the past decades, significant number of drug candidates were identified in drug discovery programs, but most of them (40–70%) are quite often poorly soluble. This challenges drug delivery institutions in industry or academia to develop innovative approaches to reach a high bioavailability after oral administration or make intravenously injectable forms available. Among these innovative formulations, lipid-based nanocarriers are an important class of carriers.

DTX, which belongs to the taxoid family, is widely used in the treatment of ovarian cancer (Kaye et al., 1997), breast cancer (Campora et al., 2008), non-small cell lung cancer (Fossella et al., 1995) and other tumors (Clarke and Rivory, 1999). However, the clinical application of DTX is limited by the poor aqueous solubility, low bioavailability and high toxicity. Presently used Taxotere® and Duopafei® in clinical contain high concentration of nonionic surfactant Tween 80. Adverse reactions due to either the drug itself or the solvent system have been reported in patients (e.g., hypersensitivity, fluid retention, neurotoxicity, musculoskeletal toxicity and neutropenia) (Chu et al., 2000). In order to eliminate the Tween 80-based vehicle and increase the drug solubility, alternative dosage forms have been developed, such as microparticulate lipoidal vesicles (liposomes) (Naik et al., 2010; Zhai et al., 2010), cyclodextrins (Grosse et al., 1998), polymeric nanoparticles (Hwang et al., 2008), micelles (Li et al., 2008), solid lipid nanoparticles (SLN) (Xu et al., 2009) and nanostructured lipid carriers (NLC) (Li et al., 2009). Among these forms, liposomes, NLC and SLN belong to lipid-based nanocarriers which have such favorable characteristics as: (a) improved drug dispersibility; (b) enhanced drug solubilization; (c) enhanced drug transmembrane transport capability and (d) increased therapeutic efficacy and reduced toxicity. In the present study, as an innovative lipid-based nanocarrier, lipid-based-nanosuspensions (LNS) have been developed. Using single injectable phospholipids as the stabilizer, LNS hold the advantages of lipid-based nanocarriers, while avoiding their shortcomings. For example, (1) LNS have no drug leakage problems, which were considered to be the common disadvantages of SLN (Müller et al., 2000; Muller et al., 2002); (2) carry adequate amounts of drug and without excessive loading of the organism with foreign material; (3) formulate compounds that are insoluble in both water and oil (Kocbek et al., 2006). Besides, (4) the drug loading of LNS is high and the administration volume is significantly reduced (Rabinow, 2004); (5) LNS is appropriate for large-scale production.

* Corresponding author. Tel.: +86 531 88382015; fax: +86 531 88382548.
E-mail address: zhangnancy9@sdu.edu.cn (N. Zhang).

0378-5173/$ – see front matter © 2011 Elsevier B.V. All rights reserved.
doi:10.1016/j.ijpharm.2011.04.023

Recently, several techniques such as precipitation methods (Sjostrom et al., 1993; Trotta et al., 2001), milling methods (Ain-Ai and Gupta, 2008) and homogenization methods (Keck and Muller, 2006) were developed to produce drug nanosuspensions. Among these methods, high pressure homogenization is the simplest one and has been successfully employed in large-scale production.

Above all, a new concept of lipid-based nanocarrier: lipid-based-nanosuspensions (LNS) were proposed. The lipid-based nanocarriers used DTX as a model drug and were produced by high pressure homogenization method. LNS were total avoidance of organic solvents during the production process, could be successfully employed for large-scale production and conveniently applied in clinical.

It has been previously reported that several DTX delivery systems such as SLN and DTX-loaded PEGylated-NPs had achieved the satisfied antitumor effect in liver cancer and colon cancer (Senthilkumar et al., 2008; Xu et al., 2009). However, the antitumor efficacy evaluation of DTX loaded nanosuspensions against malignant melanoma was rarely reported. In our study, DTX loaded LNS was first developed for murine malignant melanoma treatment. High pressure homogenization was used to the LNS preparation. The morphology, particle size and zeta potential were characterized. *In vitro* drug release was assessed using the dialysis bag diffusion technique. *In vitro* cytotoxicity of Duopafei® and LNS were performed using SKOV-3 and B16 cells. Finally, *in vivo* antitumor efficacy and the pharmacokinetics as well as the drug tissue distribution was evaluated in Kunming mice bearing B16 cells. DTX loaded LNS could avoid the serious hypersensitivity reactions caused by Tween 80 and be stable, safe and convenient for clinical administration.

2. Materials and methods

2.1. Materials

Injectable soya lecithin (phosphatidylcholine accounts for 95%, pH 5.0–7.0) was provided by Shanghai Taiwan Pharmaceutical Co., Ltd. (Shanghai, China). Duopafei® was provided by Qilu Pharmaceutical Co., Ltd. (Jinan, China). All reagents for HPLC analysis, including acetonitrile and methanol were of HPLC grade. All the other chemicals and reagents used were of analytical purity grade or higher, obtained commercially.

Human ovary cancer cells (SKOV-3) and mouse malignant melanoma (B16) cell line were obtained from Shandong Institute of Immunopharmacology and Immunotherapy (Shandong, China). 3-(4,5-Dimethylthiazol-2-yl)-2,5-diphenyl tetrazolium bromide (MTT) was purchased from Sigma–Aldrich (China).

2.2. Preparation of DTX-LNS

The DTX-LNS were prepared by high pressure homogenization. Soya lecithin (1%, w/v) was dissolved in water to obtain the aqueous surfactant solution, which was poured on the DTX (0.1%, w/v) powder and was totally mixed under high speed shearing to obtain drug suspensions. These coarse suspensions were then circulated through the high pressure homogenizer (NS1001L, Niro Soavi S.P.A., Italy) until an equilibrium size was reached.

The fresh prepared LNS were dispensed into glass vials and mannitol (5%, w/v) was added to the vials as lyoprotectant and frozen for 24 h at −80 °C. This was then transferred to a freeze-dryer (LGJ0.5, Beijing Four-Ring Scientific Instrument Co., China), and dried for 48 h at −40 °C at a pressure of 0.5 mbar to get the lyophilized DTX-LNS.

2.3. HPLC analysis of DTX

DTX concentration was measured at 230 nm by HPLC method (SPD-10Avp Shimadzu pump, LC-10Avp Shimadzu UV-vis detector). Samples were chromatographed on a 4.6 mm × 250 mm reverse phase stainless steel column packed with 5 μm particles (Venusil XBP C-18, Agela, China) eluted with a mobile phase consisting of acetonitrile/water (55:45, v/v) at a flow rate of 1.0 mL/min. The column temperature was maintained at room temperature. The samples were properly diluted by methanol and directly injected (20 μL) into the HPLC system without further treatment. The calibration curve of peak area against concentration of DTX was $A = 12,684C - 722.76$ ($r^2 = 0.9998$) under the concentration of DTX 1–50 μg/mL ($r^2 = 0.9998$, where A: peak area and C: DTX concentration) and the limit of detection was 0.02 μg/mL.

2.4. Characterization of DTX-LNS

The solution of LNS is bluish in color, which is caused by the light scattering of the nanoparticles in the solution.

The morphology of LNS was examined by transmission electron microscopy (TEM). Samples were prepared by placing a drop of fresh prepared nanosuspensions onto a copper grid and air-dried; following negative staining with a drop of 3% aqueous solution of sodium phosphotungstate for contrast enhancement (Sun et al., 2008). The Zeta potential was measured by the Laser Doppler Anemometry (LDA) on ZetaPlus Zeta Potential Analyzer (Brookheaven Instruments Corporation). And the average particle size and polydispersity index were determined by dynamic light scattering (DLS) (Zetasizer 3000SH, Malvern Instruments, UK). The lyophilized LNS were suspended with PBS (pH 7.4) before measured. All measurements were performed at 25 °C. Calculation of the size and polydispersity index was achieved using the software provided by the manufacturer. Experimental values were calculated from the measurements performed at least in triplicates.

2.5. Stability of LNS

The physical stability of the lyophilized LNS was evaluated at 4 ± 2 °C and 25 ± 2 °C. The changes in particle size and drug content were recorded over the period of 3 months.

2.6. In vitro release studies

The *in vitro* release of DTX from DTX-LNS was conducted by dialysis bag diffusion method. Lyophilized DTX-LNS, Duopafei® were suspended in 2 mL of de-ionized water (final DTX concentration, 100 μg/mL) and placed into a pre-swelled dialysis bag with 8–12 kDa molecular weight cutoff. The bag was incubated in 15 mL release medium (0.5% of Tween 80 in PBS, pH 7.4) at 37 ± 0.5 °C under horizontal shaking (Yanasarn et al., 2009). At predetermined time points, the dialysis bag was taken out and re-placed into a new container filling with 15 mL fresh medium. The amount of DTX released was determined by an HPLC method as described in Section 2.3. Sink condition was maintained throughout the release period. Data obtained in triplicate were analyzed graphically.

2.7. In vitro cytotoxicity studies

The cytotoxicity of DTX-LNS was tested in SKOV-3 and mouse B16 cells using the MTT assay (Mosmann, 1983). Briefly, cells were seeded in a 96-well plate at a density of 4000 viable cells per well and incubated for 24 h to allow cell attachment. Cells were exposed to a series of doses of Duopafei®, blank-LNS, and DTX-LNS, respectively, at 37 °C. The range of concentrations of DTX used was 0.01, 0.1, 1, 2 and 10 μM. After 96 h of incubation, 20 μL of MTT

(5 mg/mL) was added to each well of the plate. 4 h later, 200 μL/well of DMSO was added to dissolve the contents in the plate, and the absorbance of the obtained DMSO solution was measured at 570 nm and 630 nm by a microplate reader (FL600, Bio-Tek Inc., Winooski, VT). Untreated cells were taken as control with 100% viability and cells without addition of MTT were used as blank to calibrate the spectrophotometer to zero absorbance (Danhier et al., 2009).

2.8. Animals

The Kunming mice (female) weighing about 18–22 g and at the age of 6–8 weeks were used in this study, which were supplied by the Medical Animal Test Center of Shandong University. The animals were acclimatized for at least 1–2 weeks before experimentation, fed with standard diet, and allowed water ad libitum. All experiments were carried out in compliance with the Animal Management Rules of the Ministry of Health of the People's Republic of China (document no. 55, 2001) and the guidelines for the Care and Use of Laboratory Animals of China Pharmaceutical University.

2.9. In vivo antitumor efficacy

Kunming mice implanted with B16 cells were used to qualify the efficacy of DTX-LNS by i.v. The mice were subcutaneously injected at the right axillary space with 0.1 mL of cell suspension containing 5×10^4 B16 cells (Zhang et al., 2009). Treatments were started after 8–10 days of implantation. The mice with tumor volume of $\sim$100 mm^3 were selected and this day was designated as 'Day 0'. On Day 0, the mice were randomly assigned to four treatment groups, with five mice in each group. Each group of mice was treated every three days with the different formulations as described in the following: (A) DTX-LNS (DTX concentration of 20 mg/kg, diluted in physiological saline); (B) Duopafei® (dosage of 20 mg/kg, diluted in physiological saline); (C) N.S (D) blank-LNS.

All mice were labeled, and tumors were measured every other day with calipers during the period of study. The tumor volume was calculated by the formula: $V = (W^2 \times L)/2$, where W is the tumor measurement at the widest point and L the tumor dimension at the longest point. Each animal was weighed at the time of treatment, so that dosages could be adjusted to achieve the mg/kg amounts reported. Animals also were weighed every other day during the experiment period. The body weights of mice were monitored as an index of systemic toxicity (Oh et al., 2008). After 21 days, the animals were killed, and the tumor mass was harvested, weighed and photographed. The tumor inhibition ratio (TIR) could be defined as follows: TIR (%) = $((W_c - W_t)/W_c) \times 100\%$. W_c and W_t stand for the average tumor weight for control group and treatment group, respectively (Zhang et al., 2009).

2.10. Pharmacokinetics and tissue distribution

The mice with tumor were selected randomly and equally divided into two groups as subjects. Two formulations, Duopafei® and DTX-LNS were administered to the two groups respectively at a 60 mg/kg dose level via the tail vein. Blood samples which were taken from the retro-orbital plexus at predetermined time points (5, 15, 30, 45 min; 1, 2, 3, 4, 5, 6, 7and 8 h post i.v. dose), were centrifuged (4000 rpm, 15 min) and plasma was collected and stored. The mice were then euthanized by cervical dislocation, and the tumor, heart, liver, spleen, lung, kidney were collected, washed, weighed and homogenized (Ultra-turrax homogenizer (IKS T10), IKAWerke GmbH & Co., Germany) in 1 mL of physiological saline. After collection, both plasma and tissue samples were stored at −20 °C until further analysis.

2.11. Serum and tissue sample analysis

The plasma samples were extracted as previously reported. DTX plasmatic concentrations were determined as follows. Briefly, 200 μL of plasma samples was extracted by adding 250 μL methanol and 250 μL acetonitrile vortex-mixing the samples for 30 s. The mixture was then centrifuged for 15 min at 15,000 rpm, and the supernatant was transferred, filtered and injected into the HPLC system.

The tissue sample was weighed accurately and homogenized using a tissue homogenizer after addition of 1 mL physiologic saline. 200 μL tissue homogenates were processed similarly to the above disposal methods for plasma samples and analyzed by HPLC.

2.12. Pharmacokinetics and statistical analysis

The main pharmacokinetic parameters were calculated by the statistical moment method using the DAS 2.0 software. The area under the plasma concentration–time profiles (AUC), the distribution ($T_{1/2\alpha}$) and elimination half-life ($T_{1/2\beta}$), the mean residence time (MRT), and total plasma clearance (CL) were calculated. All studies were repeated a minimum of three times and measured at least in triplicate. Results were reported as means ± SD (SD: standard deviation). Statistical significance was analyzed using the Student's t-test. Differences between experimental groups were considered significant when the P-value was less than 0.05 ($P < 0.05$).

3. Results and discussion

3.1. Characterization of DTX-LNS

The DTX-LNS were homogenized applying 5, 10, 15, 20, 25 homogenization cycles at 100 MPa, respectively, and the particle diameter and polydispersity index (PI) were analyzed. The mean particle size of the suspensions decreased with the cycle number increased. There was no significant difference in the diameters of DTX-LNS between 20 cycles and 25 cycles ($P > 0.05$), while, PI of 20 cycles was smaller than that of 25 cycles ($P < 0.05$). It was indicated that both the diameter and PI were closely related to the cycle number. Based on the above results, cycle number of 20 was selected in the preparation of DTX-LNS.

The photographs of the premixed suspension before high pressure homogenization (A), the coarse DTX-LNS (B), and the DTX-LNS (C) are shown in Fig. 1. Adkins et al. (2008) had reported that an appearance of nanoparticles with particle size ranging from 50 to 200 nm showed transparent liquid. The transparent DTX-LNS obtained in the present study appear to be micronized completely from its appearance.

The TEM micrographs of the fresh-prepared DTX-LNS and the freeze-dried DTX-LNS are shown in Fig. 2. The particle diameters of the tow kinds of DTX-LNS ranged from 50 to 400 nm. The mean particle size of the fresh-prepared DTX-LNS and the freeze-dried DTX-LNS were 200.0 ± 3.42 nm and 223.3 ± 4.28 nm, respectively. The zeta potentials were −11.15 ± 0.99 mV and −10.87 ± 0.39 mV, respectively.

3.2. Stability of DTX-LNS

The physical stability of the lyophilized DTX-LNS was evaluated over 3 months at 4 ± 2 °C and 25 ± 2 °C. During this storage period, the particle size was not significantly changed and more than 99% of DTX remained in the nanosuspensions, indicating that the lyophilized product has a shelf-life of at least 3 months.

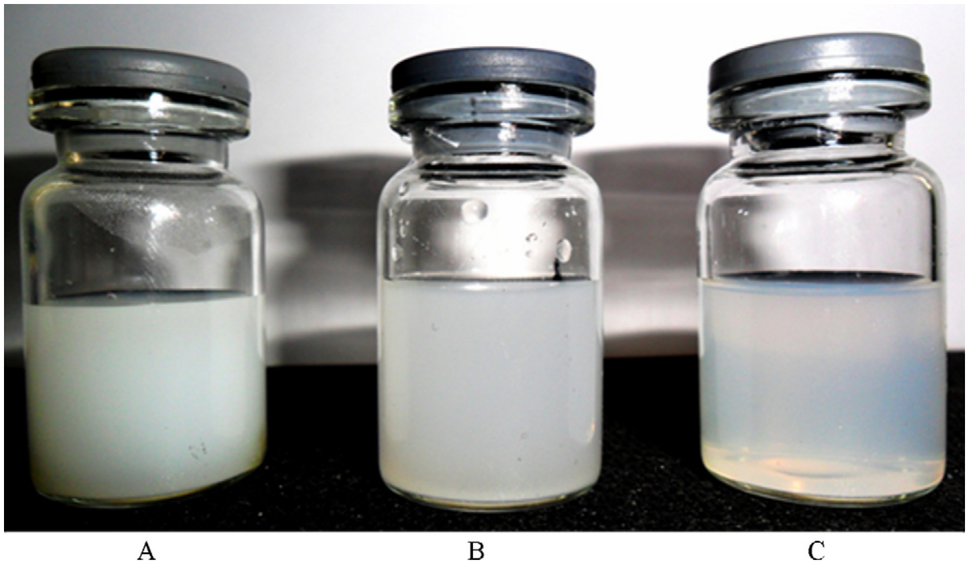

Fig. 1. Photographs of DTX-LNS: (A) premixed suspension before high pressure homogenization, (B) the coarse DTX-LNS, and (C) DTX-LNS.

3.3. *In vitro* release studies

The release experiment was conducted under sink conditions and the dynamic dialysis was employed for separation of free drug from DTX-LNS. Both the release behavior of DTX from DTX-LNS and Duopafei® followed the first-order kinetics equation and could be expressed by the following equation, respectively: for DTX-LNS: $\ln(100-Q)=-0.1961t+4.5543$, $r^2=0.9946$; for Duopafei®: $\ln(100-Q)=-0.1859t+4.4038$, $r^2=0.9991$. The release profiles of DTX-LNS and Duopafei® are shown in Fig. 3. It was obvious that DTX released from DTX-LNS was much similar to Duopafei®. Approximately 100% DTX in DTX-LNS and Duopafei ® was released within 24 h. This phenomenon could be attributed to the increased surface area of the drug and possible better contact between nanosuspensions and dissolution medium which could be favorable to the dissolution of the drug. Besides, the nanometer scale size of DTX-LNS after lyophilization could be considered to be another reason for that. According to Noyes–Whitney equation, an increase in solubility and decrease in particle size led to an increased dissolution rate (Bohm and Muller, 1999; Rebecca and Johnson, 1989).

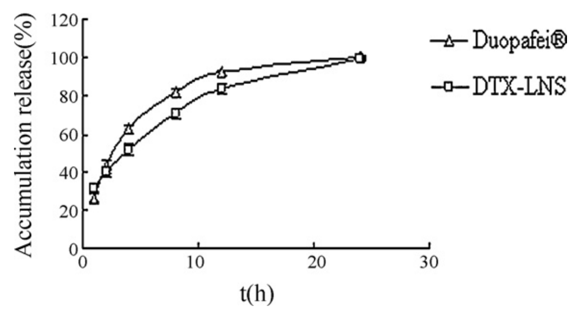

Fig. 3. *In vitro* release profile of DTX from Duopafei® and DTX-LNS in phosphate buffered saline (0.5% of Tween 80® in PBS, pH 7.4) at $37 \pm 0.5\,^{\circ}C$ ($n=3$).

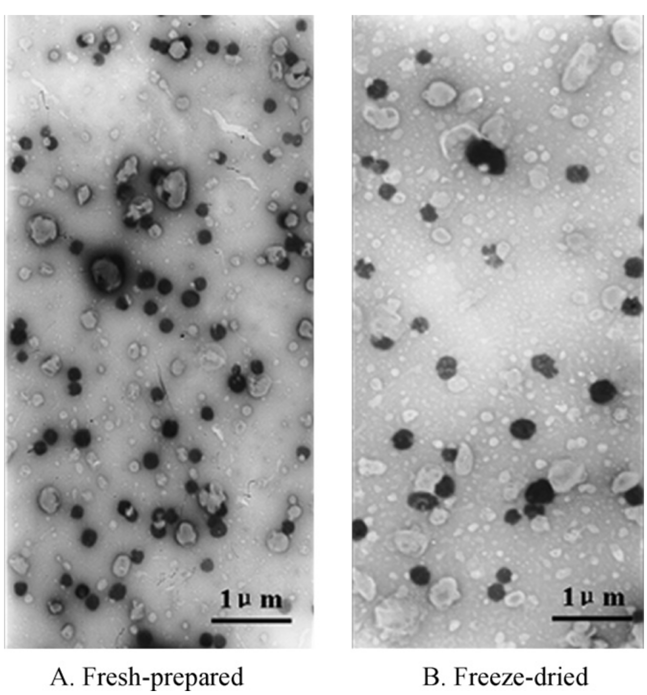

Fig. 2. Transmission electron photomicrograms of DTX-LNS: (A) fresh-prepared and (B) freeze-dried.

3.4. *In vitro* cytotoxicity

The *in vitro* cytotoxic activity of Duopafei®, blank-LNS and DTX-LNS was assessed by MTT assay in SKOV-3 and B16 cells, respectively. The half maximal inhibitory concentration (IC50) of Duopafei® and DTX-LNS for SKOV-3 and B16 ($n=3$) is presented in Table 1. It was shown that both Duopafei ® and DTX-LNS exhibited clear dose-dependent cytotoxicity against these cell lines with the concentration of loaded DTX increased from 0.01 to 10 μM. However, blank-LNS had no effects on the cell viability and showed similar result as the nontreated cells ($P>0.5$). Because the main composition of blank-LNS was soya lecithin which was a good bio-

Table 1
The IC50 of Duopafei®, DTX-LNS and blank-LNS to SKOV-3 and B16 cells. The cytotoxicity of DTX-LNS was tested in SKOV-3 and mouse B16 cells using the MTT assay and the range of concentrations of DTX used was from 0.01 to 10 μM. All the date are presented as mean ± SD ($n=3$).

Cell line	Duopafei®	DTX-LNS	Blank-LNS
SK0V-3	0.08 ± 0.04	0.08 ± 0.03	15.21 ± 0.21
B16	0.72 ± 0.10	0.69 ± 0.15	25.59 ± 1.0

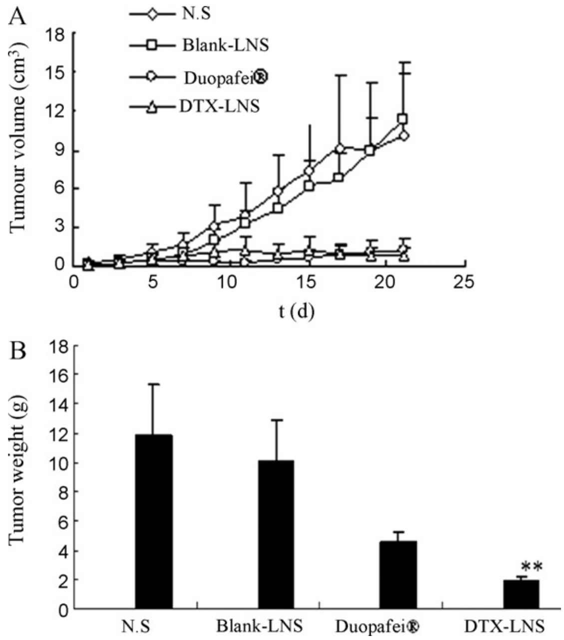

Fig. 4. Antitumor effects (in terms of tumor growth) of DTX-LNS, Duopafei®, blank-LNS and N.S on B16 tumor-bearing mice after i.v. administration. (A) Variation of tumor volume and (B) tumor weight of each treatment group. $^{**}P < 0.01$, compared with Duopafei®. Data were given as mean ± SD ($n = 5$).

compatible material, could be totally metabolized and non-toxic to cells. Therefore, the cytotoxicity of Duopafei® and DTX-LNS could be attributed to the toxic effects of DTX. With the concentration increased, the toxicity enhanced, which suggested that the drug concentration played a major role in the *in vitro* cytotoxicity of DTX. These results also indicated that the cytotoxicity of drug-loaded nanoparticles was nearly the same as that of free drug. Similar results were also reported in the previous studies (Li et al., 2008; Zhang et al., 2004, 2007).

3.5. In vivo antitumor effect

The *in vivo* antitumor effects of DTX-LNS were assessed using B16 bearing mice as the model animals. Fig. 4(A) depicts the changes of tumor volume and the weights of excised tumor mass are shown in Fig. 4(B). It was found that the tumor volumes of DTX-LNS group were smaller than those of Duopafei® group after injection two weeks ($P < 0.05$) and significant differences in tumor weights were observed between Duopafei® groups and the groups receiving DTX-LNS at the same dose ($P < 0.01$), indicating that DTX-LNS could effectively inhibit tumor growth, while no antitumor effect was observed in the group of N.S and blank-LNS. As shown in Fig. 5, these typical photographs of excised sarcomas from the tested groups provide a direct visual representation of the tumor suppression effect.

The tumor inhibition rates of DTX-LNS and Duopafei® group compared with N.S group are listed in Table 2. The DTX-LNS group showed more significant tumor inhibition rate (84.51 ± 3.49)% than Duopafei® (62.17 ± 6.45)% ($P < 0.01$).

Fig. 6 depicts the variation of relative body weight of the mice. These results suggested that the mice experienced a large weight increase from the day of the administration of different formulations to the end of the experiment. These increases were 18.58%, 51.50% and 37.80% for N.S, blank-LNS and DTX-LNS, respectively. But the body weight of the group treated with Duopafei® experienced a slight weight loss (less than 10%). This weight loss induced by Duopafei® was much significant than those induced by DTX-LNS ($P < 0.01$). The analysis of body weight variations could be used to

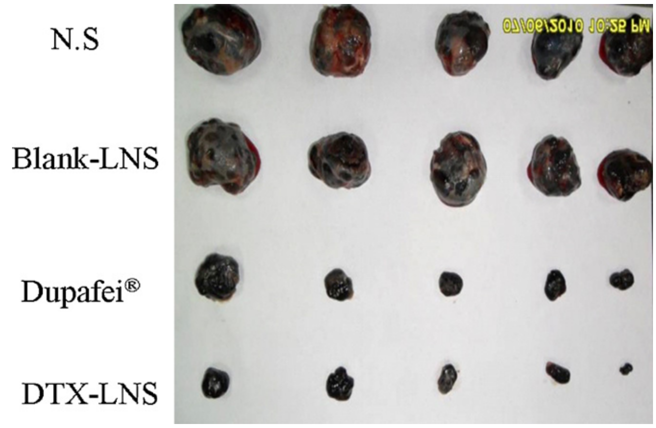

Fig. 5. Photographs of tumors from each treatment group excised on Day 21. Data were given as mean ± SD ($n = 5$).

define the adverse effects of the different therapy regiments (Zheng et al., 2009). It could be concluded that that DTX-LNS exhibited less toxicity to mice than Duopafei®. Therefore, it would facilitate the clinical application of DTX-LNS when administered intravenously under the present experiment condition. Moreover, it was observed that the mice of Duopafei® group were in a weak state in the aspects of movement and spirit and two mice died during the experiment, whereas no obvious alteration was observed in the DTX-LNS group. It could be speculated that the tumor inhibition ability of DTX-LNS increased survival rates of B16 bearing mice. Thus, nanosized drug carriers possess advantages of reducing the high dose dependent toxicity of anticancer drugs while, simultaneously increasing their anticancer efficacy (Hwang et al., 2008).

To further verify the lower toxicity of DTX-LNS compared with Duopafei®, twenty B16 bearing mice were used as the model animals in the following study. Among the 10 mice injected with 20 mg/kg Duopafei®, one mouse died after 10 days, and 7 other mice died within 35 days. It was likely due to the high toxic effects of free DTX and the solvent system. In contrast, the other 10 mice treated with 20 mg/kg DTX-LNS were all alive after 35 days. It could be concluded that DTX-LNS could increase survival rates by reducing *in vivo* toxicity of normal tissues.

Overall, these findings indicated that DTX-LNS showed higher efficacy and much lower side effects in B16 bearing mice model compared with Duopafei®, which could be attributed to following reasons. Firstly, DTX-loaded LNS showed much better toleration *in vivo* compared with Duopafei®. Efficacy and therapeutic value of DTX could be substantially diminished by severe systemic toxicity. Cytotoxic drugs typically show a steep dose–response curve and high dose intensity was required to ensure therapeutic success, which led to a dilemma between high drug dose with high

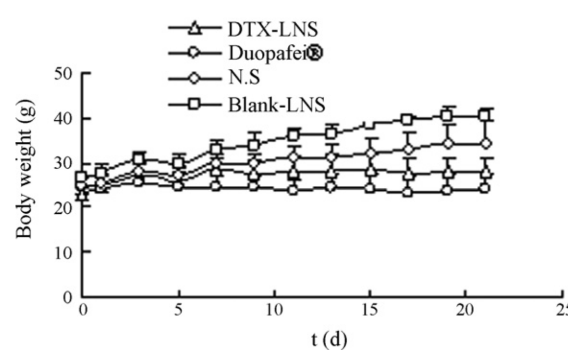

Fig. 6. Body weight change observed in B16-tumor bearing mice treated with different formulations. Data were given as mean ± SD ($n = 5$).

Table 2
The TIR of DTX-LNS and Duopafei® group.

Groups	Dose (mg/kg)	Animals number (start/end)	Average tumor weight (g)	TIR (100%)
N.S	–	10/10	11.86 ± 3.46	–
DTX-LNS	20	10/10	1.84 ± 0.41	84.51 ± 3.49**,##
Duopafei®	20	10/8	4.49 ± 0.77	62.17 ± 6.45**

** $P<0.01$ vs. N.S.
$P<0.01$ vs. Duopafei®

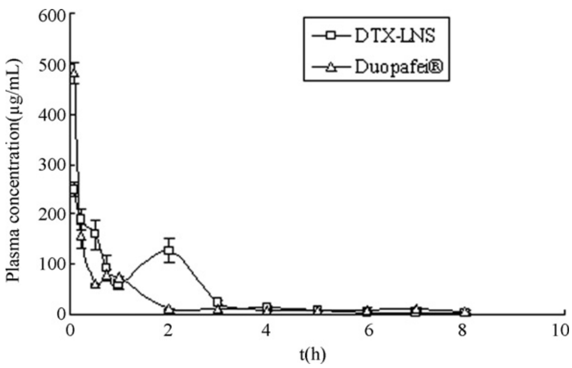

Fig. 7. The mean plasma concentration–time curves of DTX in B16-bearing mice after a single i.v. dose (60 mg/kg) of Duopafei® and DTX-LNS, the data were presented as mean ± SD ($n=4$).

Table 3
Plasma pharmacokinetic parameters after i.v. of Duopafei® and DTX-LNS at a dose of 60 mg/kg of DTX (mean ± SD, $n=4$).

Pharmacokinetic parameters	Formulations	
	Duopafei®	DTX-LNS
C_{max} (μg/mL)	481.62 ± 13.23	248.58 ± 21.19**
$T_{1/2\alpha}$ (h)	0.31 ± 0.06	0.13 ± 0.05
$T_{1/2\beta}$ (h)	1.78 ± 0.11	3.29 ± 0.18*
$AUC_{0-\infty}$ (mg/L h)	308.42 ± 20.23	404.05 ± 26.19**
MRT (h)	1.76 ± 0.15	3.37 ± 0.22*

* $P<0.05$ vs. Duopafei®.
** $P<0.01$ vs. Duopafei®.

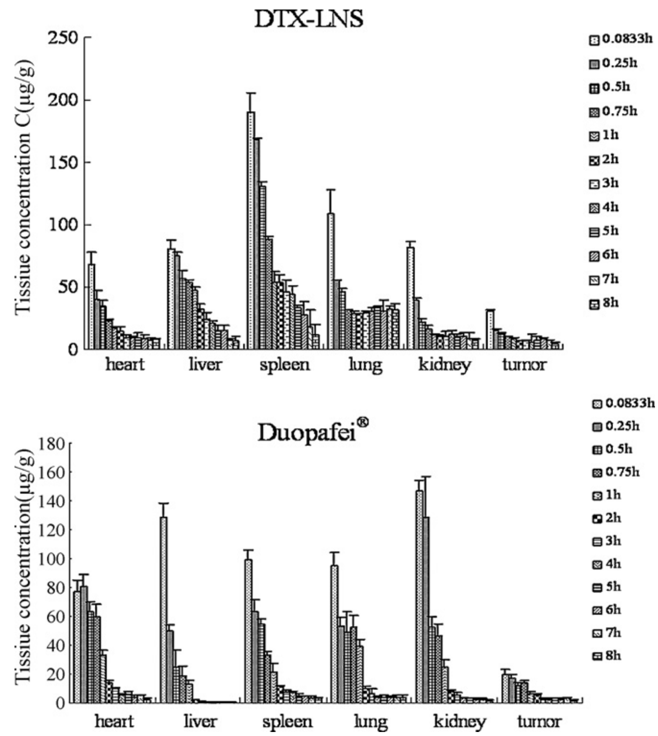

Fig. 8. Concentrations of DTX in different tissues at 8 h following i.v. of Duopafei® and DTX-LNS of 60 mg/kg to B16 bearing mice ($n=4$).

risk of normal tissue toxicity and low drug dose with low therapeutic effect (Wong et al., 2007). In addition, only when the cytotoxic anticancer drug reached the tumor could it exert therapeutic effect. It could be speculated that compared with Duopafei®, DTX-loaded LNS resulted in higher accumulation in both the liver and the tumor. LNS could increase drug concentration in tumor via the enhanced permeability and retention (EPR) effect. To prove our speculation, biodistribution studies were carried out.

3.6. Pharmacokinetics and tissue distribution

The standard curves having DTX concentrations ranging from 0.5 to 50 μg/mL exhibited good linearity and correlation coefficients over this concentration range were 0.9994–0.9999 for plasma and all measured organs.

I.v. administration of both Duopafei® and DTX-LNS was well tolerated by all B16 tumor-bearing mice. The plasma concentration–time profiles of DTX of Duopafei® and DTX-LNS are shown in Fig. 7 and the corresponding pharmacokinetic parameters are in Table 3. Although both plasma profiles were found to be fitted with the two-compartment model, DTX-LNS exhibiting a very rapid distribution phase ($T_{1/2\alpha}=0.13\pm0.05$ h) compared to Duopafei® ($T_{1/2\alpha}=0.31\pm0.06$ h). The peak plasma concentration (C_{max}) achieved from Duopafei® (481.62 ± 13.23 μg/mL) was significantly higher ($P<0.01$) than that from DTX-LNS (248.58 ± 21.19 μg/mL). The plasma $AUC_{0-\infty}$ of DTX-LNS (404.05 ± 26.19 mg/L h) was approximately 1.31-fold greater than that of Duopafei® (308.42 ± 20.23 mg/L h), and overall the mean residence time (MRT, 3.37 ± 0.22 h) for the DTX-LNS formulation was considerably longer (1.92-fold) than that observed for the Duopafei®. These results indicted that the plasma pharmacokinetics of DTX given in the LNS formulation were different from Duopafei®. It was reported the uptake of nanoparticles by RES organs following intravenous injection might taken from a few minutes to hours, depending on the particle size and composition (Manjunath and Venkateswarlu, 2005). The DTX nanoparticles uptaken by RES, might dissolve slowly in phagocytic cell and release into blood circulation, and remain a longer blood level compared with Duopafei®.

In contrast to the plasma profiles, in all tissues (except the heart and kidney), significantly higher DTX concentrations in DTX-LNS group were observed in B16 tumor-bearing mice compared with Duopafei® ($P<0.01$) (Fig. 8). For both DTX-LNS and Duopafei® group, the highest level of DTX in all the collected tissues was observed at 5 min after i.v. administration. $AUC_{(0-8\,h)}$ and $MRT_{(0-8\,h)}$ values of tested organs for the two formulations are given in Table 4. The $AUC_{(0-8\,h)}$ and $MRT_{(0-8\,h)}$ values of DTX-LNS were found to be much higher than that of Duopafei® in liver, spleen and lung ($P<0.01$). It could be explained that these nanosuspensions had a relatively large mean diameter (223.3 ± 4.28 nm). They could circulate in the blood as submicron particles for a certain time period, and then they might be recognized as foreign matters and rapidly cleared by phagocytic cells of mononuclear phagocyte sys-

Table 4
Average pharmacokinetic parameters ($n = 4$) of DTX after i.v. of Duopafei®, DTX-LNS to B16 bearing mice with dose of 60 mg/kg.

	$AUC_{(0-8)}$ (mg/L h)	$MRT_{(0-8)}$ (h)
DTX-LNS		
Heart	77.92 ± 5.36**	1.37 ± 0.02**
Liver	220.05 ± 23.43**	2.58 ± 0.16**
Spleen	394.41 ± 32.11**	2.63 ± 0.15**
Lung	250.76 ± 20.41**	3.78 ± 0.12**
Kidney	102.05 ± 4.64**	1.19 ± 0.07**
Tumor	53.259 ± 3.63*	5.20 ± 0.97**
Duopafei®		
Heart	134.07 ± 10.13	1.86 ± 0.08
Liver	47.49 ± 8.90	0.89 ± 0.05
Spleen	104.59 ± 4.62	1.88 ± 0.07
Lung	107.65 ± 8.82	1.88 ± 0.21
Kidney	141.52 ± 19.27	3.26 ± 0.24
Tumor	38.07 ± 1.40	2.69 ± 0.05

* $P < 0.05$ compared with Duopafei®.
** $P < 0.01$ compared with Duopafei®.

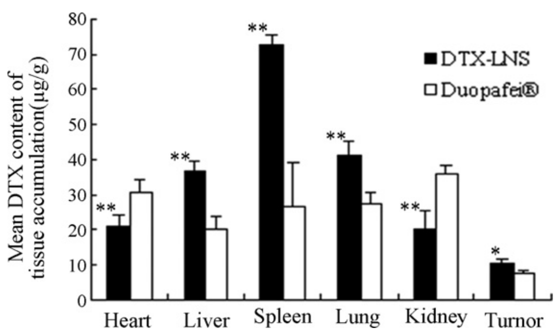

Fig. 9. Mean DTX content of heart, liver, spleen, lung, kidney and tumor after i.v. of Duopafei® and DTX-LNS. *$P < 0.05$, **$P < 0.01$ compared with Duopafei®.

tem (MPS) which abounded in special tissues and organs, such as liver, lung and spleen (Gao et al., 2008). Therefore, DTX-LNS had a markedly higher concentration compared with Duopafei ® in these organs, meanwhile the drug concentration in heart and kidney decreased. Similar results were reported by Peters et al. (2000).

The mean DTX contents of heart, liver, spleen, lung, kidney and tumor after i.v. of two formulations are shown in Fig. 9. For DTX-LNS group, 18.31%, 36.09% and 20.60% DTX were distributed in liver, spleen and lung, respectively. Compared with the amount of DTX accumulated within the organs rich in macrophages (liver, lungs and spleen), the amount of drug targeted to tumor was lower. In order to reach all viable cells in the tumor, anticancer drugs must be delivered efficiently through the tumor vasculature, cross the vessel wall, and traverse the tumor tissue (Tredan et al., 2007). Therefore, nanosuspensions targeted to tumor by EPR (enhanced permeability and retention) effect might be relatively difficult. Nevertheless, nanoparticles could be engulfed by MPS rapidly to increase the drug concentration in liver. The passive targeting of DTX-LNS to liver might suggest an enhanced therapeutic effect on liver cancers, and it still needs further investigation.

4. Conclusion

In the present study, DTX-LNS were successfully prepared by high pressure homogenization. Compared with Duopafei®, DTX-LNS showed higher antitumor efficacy, increased survival rate in B16 cells bearing mice and strongly reduced anticancer drug toxicity. So we have applied for patents to protect our achievement (Wang et al., 2010).

Above all, LNS were total avoidance of organic solvents during the production process, could be successfully employed for large-scale production and conveniently applied in clinical.

In our future work, we will warrant more strict research in order to further research the *in vivo* antitumor effect and toxicity of the DTX-LNS. We will also focus on the development of stealth and active targeting LNS carriers modified with functionalized surface coatings, and ultimately, the feasibility and advantages of clinical applications.

Acknowledgement

The authors are grateful to R & D projects in key areas of Jining City for providing financial assistance to carry out this work.

References

Adkins, S.S., Hobbs, H.R., Benaissi, K., Johnston, K.P., Poliakoff, M., Thomas, N.R., 2008. Stable colloidal dispersions of a lipase-perfluoropolyether complex in liquid and supercritical carbon dioxide. J. Phys. Chem. B 112, 4760–4769.

Ain-Ai, A., Gupta, P.K., 2008. Effect of arginine hydrochloride and hydroxypropyl cellulose as stabilizers on the physical stability of high drug loading nanosuspensions of a poorly soluble compound. Int. J. Pharm. 351, 282–288.

Bohm, B.H., Muller, R.H., 1999. Lab-scale production unit design for nanosuspensions of sparingly soluble cytotoxic drugs. Pharm. Sci. Technol. Today 2, 336–339.

Campora, E., Colloca, G., Ratti, R., Addamo, G., Coccorullo, Z., Venturino, A., Guarneri, D., 2008. Docetaxel for metastatic breast cancer: two consecutive phase II trials. Anticancer Res. 28, 3993–3995.

Chu, C.Y., Yang, C.H., Yang, C.Y., Hsiao, G.H., Chiu, H.C., 2000. Fixed erythrodysaesthesia plaque due to intravenous injection of docetaxel. Br. J. Dermatol. 142, 808–811.

Clarke, S.J., Rivory, L.P., 1999. Clinical pharmacokinetics of docetaxel. Clin. Pharmacokinet. 36, 99–114.

Danhier, F., Lecouturier, N., Vroman, B., Jerome, C., Marchand-Brynaert, J., Feron, O., Preat, V., 2009. Paclitaxel-loaded PEGylated PLGA-based nanoparticles: in vitro and in vivo evaluation. J. Control. Release 133, 11–17.

Fossella, F.V., Lee, J.S., Shin, D.M., Calayag, M., Huber, M., Perez-Soler, R., Murphy, W.K., Lippman, S., Benner, S., Glisson, B., et al., 1995. Phase II study of docetaxel for advanced or metastatic platinum-refractory non-small-cell lung cancer. J. Clin. Oncol. 13, 645–651.

Gao, L., Zhang, D., Chen, M., Duan, C., Dai, W., Jia, L., Zhao, W., 2008. Studies on pharmacokinetics and tissue distribution of oridonin nanosuspensions. Int. J. Pharm. 355, 321–327.

Grosse, P.Y., Bressolle, F., Pinguet, F., 1998. In vitro modulation of doxorubicin and docetaxel antitumoral activity by methyl-beta-cyclodextrin. Eur. J. Cancer 34, 168–174.

Hwang, H.Y., Kim, I.S., Kwon, I.C., Kim, Y.H., 2008. Tumor targetability and antitumor effect of docetaxel-loaded hydrophobically modified glycol chitosan nanoparticles. J. Control. Release 128, 23–31.

Kaye, S.B., Piccart, M., Aapro, M., Francis, P., Kavanagh, J., 1997. Phase II trials of docetaxel (Taxotere (R)) in advanced ovarian cancer—an updated overview. Eur. J. Cancer 33, 2167–2170.

Keck, C.M., Muller, R.H., 2006. Drug nanocrystals of poorly soluble drugs produced by high pressure homogenisation. Eur. J. Pharm. Biopharm. 62, 3–16.

Kocbek, P., Baumgartner, S., Kristl, J., 2006. Preparation and evaluation of nanosuspensions for enhancing the dissolution of poorly soluble drugs. Int. J. Pharm. 312, 179–186.

Li, X., Li, R., Qian, X., Ding, Y., Tu, Y., Guo, R., Hu, Y., Jiang, X., Guo, W., Liu, B., 2008. Superior antitumor efficiency of cisplatin-loaded nanoparticles by intratumoral delivery with decreased tumor metabolism rate. Eur. J. Pharm. Biopharm. 70, 726–734.

Li, X., Wang, D., Zhang, J., Pan, W., 2009. Preparation and pharmacokinetics of docetaxel based on nanostructured lipid carriers. J. Pharm. Pharmacol. 61, 1485–1492.

Müller, R.H., et al., 2000. Solid-lipid(semi-solid) lipid particles and method of producing highly concentrated lipid particle dispersions, German.

Manjunath, K., Venkateswarlu, V., 2005. Pharmacokinetics, tissue distribution and bioavailability of clozapine solid lipid nanoparticles after intravenous and intraduodenal administration. J. Control. Release 107, 215–228.

Mosmann, T., 1983. Rapid colorimetric assay for cellular growth and survival: application to proliferation and cytotoxicity assays. J. Immunol. Methods 65, 55–63.

Muller, R.H., Radtke, M., Wissing, S.A., 2002. Nanostructured lipid matrices for improved microencapsulation of drugs. Int. J. Pharm. 242, 121–128.

Naik, S., Patel, D., Surti, N., Misra, A., 2010. Preparation of PEGylated liposomes of docetaxel using supercritical fluid technology. J. Supercrit. Fluids 54, 110–119.

Oh, K.T., Lee, E.S., Kim, D., Bae, Y.H., 2008. L-Histidine-based pH-sensitive anticancer drug carrier micelle: reconstitution and brief evaluation of its systemic toxicity. Int. J. Pharm. 358, 177–183.

Peters, K., Leitzke, S., Diederichs, J.E., Borner, K., Hahn, H., Muller, R.H., Ehlers, S., 2000. Preparation of a clofazimine nanosuspension for intravenous use and evaluation of its therapeutic efficacy in murine *Mycobacterium avium* infection. J. Antimicrob. Chemother. 45, 77–83.

Rabinow, B.E., 2004. Nanosuspensions in drug delivery. Nat. Rev. Drug Discov. 3, 785–796.

Rebecca, J.H., Johnson, K.C., 1989. The effect of particle size distribution on dissolution rate and oral absorption. Int. J. Pharm. 51, 9–17.

Senthilkumar, M., Mishra, P., Jain, N.K., 2008. Long circulating PEGylated poly (D, L-lactide-co-glycolide) nanoparticulate delivery of Docetaxel to solid tumors. J. Drug Target 16, 424–435.

Sjostrom, B., Bergenstahl, B., Kronberg, B., 1993. A method for the preparation of submicron particles of sparingly water-soluble drugs by precipitation in oil-in-water emulsions. II: influence of the emulsifier, the solvent, and the drug substance. J. Pharm. Sci. 82, 584–589.

Sun, W., Zhang, N., Li, A., Zou, W., Xu, W., 2008. Preparation and evaluation of N(3)-O-toluyl-fluorouracil-loaded liposomes. Int. J. Pharm. 353, 243–250.

Tredan, O., Galmarini, C.M., Patel, K., Tannock, I.F., 2007. Drug resistance and the solid tumor microenvironment. J. Natl. Cancer Inst. 99, 1441–1454.

Trotta, M., Gallarate, M., Pattarino, F., Morel, S., 2001. Emulsions containing partially water-miscible solvents for the preparation of drug nanosuspensions. J. Control. Release 76, 119–128.

Wang, L.L., et al., 2010. A method of producing lyophilized Docetaxel nanocrystalline, China.

Wong, H.L., Bendayan, R., Rauth, A.M., Li, Y., Wu, X.Y., 2007. Chemotherapy with anticancer drugs encapsulated in solid lipid nanoparticles. Adv. Drug Deliv. Rev. 59, 491–504.

Xu, Z., Chen, L., Gu, W., Gao, Y., Lin, L., Zhang, Z., Xi, Y., Li, Y., 2009. The performance of docetaxel-loaded solid lipid nanoparticles targeted to hepatocellular carcinoma. Biomaterials 30, 226–232.

Yanasarn, N., Sloat, B.R., Cui, Z.R., 2009. Nanoparticles engineered from lecithin-in-water emulsions as a potential delivery system for docetaxel. Int. J. Pharm. 379, 174–180.

Zhai, G.X., Wu, J., Yu, B., Guo, C.Y., Yang, X.G., Lee, R.J., 2010. A transferrin receptor-targeted liposomal formulation for docetaxel. J. Nanosci. Nanotechnol. 10, 5129–5136.

Zhang, J., Qian, Z., Gu, Y., 2009. In vivo anti-tumor efficacy of docetaxel-loaded thermally responsive nanohydrogel. Nanotechnology 20, 325102.

Zhang, L., Hu, Y., Jiang, X., Yang, C., Lu, W., Yang, Y.H., 2004. Camptothecin derivative-loaded poly (caprolactone-co-lactide)-b-PEG-b-poly (caprolactone-co-lactide) nanoparticles and their biodistribution in mice. J. Control. Release 96, 135–148.

Zhang, L., Yang, M., Wang, Q., Li, Y., Guo, R., Jiang, X., Yang, C., Liu, B., 2007. 10-Hydroxycamptothecin loaded nanoparticles: preparation and antitumor activity in mice. J. Control. Release 119, 153–162.

Zheng, D., Li, X., Xu, H., Lu, X., Hu, Y., Fan, W., 2009. Study on docetaxel-loaded nanoparticles with high antitumor efficacy against malignant melanoma. Acta Biochim. Biophys. Sin. (Shanghai) 41, 578–587.